



## Materials Analysis Using Synchrotron Radiation

Yoshiharu Hirose

### Abstract

Synchrotron radiation (SR) is a tunable, highly oriented, intense X-ray. Its tunability has led to XAFS being used as a common analytical tool, and is particularly useful for examining local structures. In fact, its use is indispensable to the examination of not only amorphous materials or solutions but also multi-component systems. Thanks to the high intensity of SR, it is possible to determine the structure or composition of very small areas or monolayers. Researchers who are faced with difficulties caused by the limits of conventional experimental techniques would be well advised to consider X-ray analysis using SR.

Keywords

Synchrotron radiation, X-ray diffraction, XAFS, Micro beam

---

## 1. Introduction

---

More and more studies are relying on synchrotron radiation (SR) as an analytical tool. Of course, SR is not a prerequisite for materials research. In fact, conventional X-ray techniques are still providing researchers with useful results. But, any researcher who faces difficulties caused by the limits imposed by conventional techniques would be well advised to consider the use of SR. While many books and review articles about the use of SR in materials research have been published<sup>1-12)</sup>, in this paper we would like to introduce SR to those researchers who are still relying on X-ray equipment as their main analytical tools. In particular, I would like to emphasize the new possibilities that SR brings to materials research. If you would like to learn more about SR, refer to the references given at the end of this paper, or use the keywords given above to perform an Internet search. I hope that this article will provide you with some pointers to further advance your materials research.

---

## 2. Characteristics of synchrotron radiation

---

Synchrotron radiation (SR) is the light that is emitted by electrons when they are accelerated to a velocity close to the speed of light and then their orbits are changed by a magnetic field. A facility for generating of SR consists of an electron accelerator, a storage ring and beam-lines. Electrons are accelerated up to the given energy (hundreds of MeV to the GeV order) by the accelerator and are then injected into the synchrotron. The latter is referred to as a "storage ring". Electrons are injected as pulses with a time width of around 0.1 nsec. Each group of electron pulses is called a "bunch". The bunches travel around the storage rings with a period in the order of microseconds. Bending magnets determine the orbit of the electrons within the storage ring. In so-called "third generation" SR facilities, insertion devices known as "wigglers" or "undulators" are installed in the straight section between the bending magnets. The light is then emitted through either the bending magnet or the insertion devices, and conducted to the beam-lines.

The light emitted from the bending magnet has a continuous spectrum, ranging from electric waves to

hard X-rays. The spectrum peak depends on the energy of the storage ring and the strength of the magnetic field. In so-called "third generation" SR facilities, it is in the hard X-ray region. The wigglers are intended to produce light with a higher energy (shorter wave length), but with a spectrum resembling that obtained with the bending magnets. The undulators, on the other hand, are used to produce more intense light, with a pseudo-monochromatic rather than a continuous spectrum. The gap between the magnets inside the undulator can be varied to control the peak energy. In a normal beam-line, the light is monochromatized by a monochromator, although some beam-lines use white light without a monochromator. **Table 1** lists some of the characteristic properties of SR facilities. At present, the Japanese SPring-8 is the largest third generation SR facility in the world in terms of electron energy held in the storage ring. In summing up, SR lights are tunable, highly oriented, and intense X-rays.

---

## 3. Diffraction

---

### 3.1 Powder X-ray diffraction

X-ray diffraction patterns with a high S/N ratio can be obtained by using SR light because of its excellent monochromaticity and high brilliance. Weak diffraction peaks, which previously could barely be observed in the laboratory, appear as a distinct peak. Therefore, SR is superior for powder X-ray crystal structure determination using the Rietveld method, when compared with conventional laboratory.<sup>13)</sup>

In the beam-line of BL02B2 (SPring-8), an incident beam with a diameter of 1 mm is applied to the sample that is held in a glass capillary tube with a diameter that is less than the beam size. The diffraction pattern is recorded on a cylindrically bent imaging plate. Fine crystal structure refinement using the Rietveld method is possible in a beam-line having this configuration, because the absorption and preferential orientation are negligible, and the superior dynamic range of the imaging plate ensures that we can observe high-quality diffraction peaks. Furthermore, combining the Rietveld method with the maximum entropy method (MEM) provides us with details of the electronic density distribution

such as bonding electrons or the electron density around the light elements in a crystal. For example, Takata et al.<sup>14-15)</sup> performed a crystal structure analysis of metallofullerenes, in which metal atoms are encapsulated within a carbon cage. They not only evaluated the valences of the metal, but also found that the metal atoms in a metallofullerene form a cluster. They also discovered C<sub>66</sub>, which cannot exist in nature in its empty form due to the isolated-pentagon rule, but can exist if encapsulating a cluster of Sc<sub>2</sub>.

Due to the energy tunability of SR, the application of the anomalous dispersion effect, which involves an abrupt change in the atomic scattering factor at the absorption edge of the atom, has become widely used to determine the position of atoms in metallic alloys and mixed oxides.

### 3.2 Single-crystal X-ray structure analysis

For single-crystal X-ray structure analysis, the data acquisition time can be shortened by making use of the brilliance of SR and a two-dimensional detector such as a CCD and an imaging plate. Given the energy tunability of SR, the multi-wavelength anomalous dispersion (MAD) technique has been

widely applied to the phase determination of protein crystal structures. Because of the enthusiasm for drug design in the post-sequence era, almost all SR facilities are at least partially used for determining protein structures.

### 3.3 Surface X-ray diffraction

Glazing incidence X-ray diffraction (GIXRD) is a technique for observing crystal phases in surface layers. Diffracted X-rays are detected by the  $2\theta$  scan while the sample is held with a small angle between the incident X-ray and its surface. This technique is commonly used in laboratories. SR becomes necessary, however, if the sample's surface layer is so thin that it can only produce very little diffraction. The in-plane diffraction method, which can be used to observe crystal planes lying perpendicular to the surface, is necessary for specimens in which the crystals are preferentially oriented. In the liquid-crystal/polyimide/substrate systems used in flat-panel displays, the buffing of the polyimide films with a cloth produces liquid-crystal alignment in the rubbing direction. In-plane GIXRD with SR clearly shows whether the scattering vector  $q$  is parallel or perpendicular to the

**Table 1** Some Characteristics of SR facilities.

	Ritsu SR <sup>a)</sup>	UVSOR <sup>b)</sup>	PF <sup>c)</sup>	ESRF <sup>d)</sup>	APS <sup>e)</sup>	SPring-8 <sup>f)</sup>
Energy (GeV)	0.575	0.75	2.5	6.03	7.0	8.0
Current (mA) (max)	300	200 (500)	400 (770)	200	100 (300)	100
Circumference (m)	3.14	53.2	187	844	1,104	1,436
Number of beam lines	14	16	21	56	68	61
Available year	1996	1984	1982	1994	1996	1997

a) SR Center, Ritsumeikan Univ., Kusatsu, Japan

b) UVSOR, Institute for Molecular Science, Okazaki, Japan

c) Photon Factory, Tsukuba, Japan

d) European Synchrotron Radiation Facility, Grenoble, France

e) Advanced Photon Source, Argonne, The U.S.A.

f) Super Photon Ring, Mikazuki, Japan

rubbing direction.<sup>9)</sup> It has been shown that the alignment of liquid-crystals reflects a template, which is formed by the buffing of the polyimide surface.

Robinson<sup>16)</sup> pointed out that the abrupt termination of a three-dimensional crystal at its surface produces a diffraction intensity between the reciprocal lattice points as shown in **Fig. 1**. He named these "crystal truncation rods" (CTR). The intensity along  $q_{\perp}$ , which can be obtained by changing the incident angle, depends on the surface roughness and the interference caused by the substrate. The power of SR was demonstrated by means of CTR analysis, where  $10^5$  dynamic ranges are necessary to observe the CTR effect. Tabuchi et al.<sup>17)</sup> revealed the role of the AlN buffer layer between GaInN and sapphire. The use of X-rays is a very unique means of investigating such a buried layer.

To investigate the surface structure, electron diffraction such as low-energy electron diffraction (LEED) and reflection high-energy electron diffraction (RHEED) has been used.<sup>18)</sup> To quantitatively examine the intensity, one must consider multiple scattering (dynamical theory), when using electron diffraction. On the other hand, single scattering (kinematical theory) is sufficient to handle the intensity with X-ray scattering. This is an

advantage of surface X-ray diffraction (SXRD). These GIXRD, SXRD, and CTR methods are collectively referred to as surface X-ray scattering (SXRS).

### 3.4 X-ray reflectivity

The X-ray reflectivity method is often used in the laboratory like GIXD. **Figure 2** is a schematic of the reflectivity curves for an ideal smooth surface, a surface with roughness, and a smooth monolayer, where  $\alpha_c$  denotes the critical angle for the total

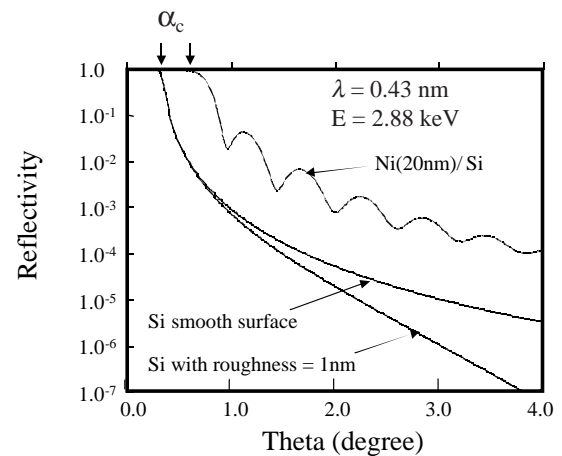
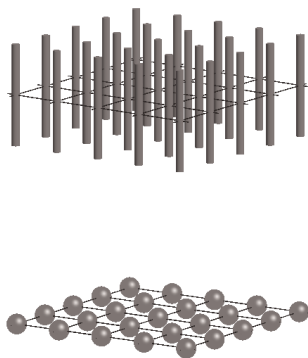
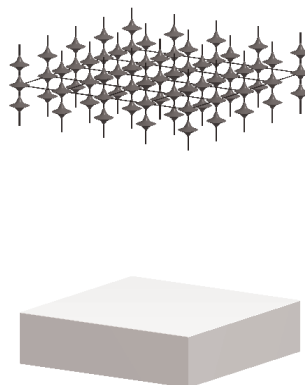


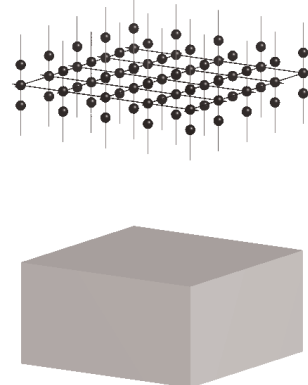
**Fig. 2** X-ray reflectivity.



(a) An ideal 2-dim. Crystal (below).  
r-space consists of rods (above).



(b) Real surface truncated at the  
surface (below).  
r-space consists of CTR (above).



(c) Bulk crystal (below).  
r-space consists of points (above).

**Fig. 1** Crystal truncation rods (CTR).

reflection. Since the refractive indexes for the usual substances are slightly less than 1, the incident X-rays are totally reflected when the incident angle is less than  $\alpha_c$ . The oscillation is the result of interference between of the reflection from the top of the surface and that from the interface between the monolayer and the substrate (Kiessig structure).

Sources within the semiconductor industry predict that gate oxide thicknesses will fall to less than 1 nm by 2005.<sup>21)</sup> Such thinner layers will result in longer periods and larger amplitude changes in the oscillation. Therefore, the high brilliancy of SR would be even more advantageous. Awaji et al.<sup>22)</sup> characterized a monolayer with a thickness of 0.3 nm by using a diffractometer in BL16XU (SPring-8). Using X-ray reflectivity methods, information about the atomic composition is difficult to obtain, especially when the materials have similar atomic numbers and densities and hence have similar refractive indices. Awaji developed a grazing incidence X-ray fluorescence (GIXRF) technique that is based on the matrix formalism of reflectivity. This technique allows the intensities of both the reflectivity and fluorescence to be analyzed simultaneously.<sup>23)</sup>

### 3.5 X-ray stress analysis

X-ray stress analysis is a technique for determining the amount of residual stress by observing the strain  $\Delta d/d$  ( $d$  denotes the spacing of the crystal plane). In laboratory experiments, Co  $K\alpha$  (0.179 nm, 6.93 keV) is often used. The penetration depth of the Co  $K\alpha$  X-rays is 48  $\mu\text{m}$  in the case of Al, and 22  $\mu\text{m}$  for Fe, which corresponds to the maximum depth to which we can observe residual stress. On the other hand, hard X-rays allow us to obtain more internal information about the specimen (for example to a depth of 15 mm for Al and 2 mm for Fe at 60 keV). Neutron diffraction can also be applied to residual stress measurement. The main advantage of this method is that it provides more internal information than regular X-ray techniques. However, the volume of the specimen must be larger than the X-ray beam. Reimers et al.<sup>24)</sup> measured the stress distribution in a turbine blade (Ni-based alloy, with a thickness of 2 mm) with an Yttria-stabilized zirconia (YSZ) thermal barrier coating (0.5 mm thick) under a four-point bending test in ID15A

(ESRF). Both the glancing incidence and micro beam techniques have been applied to obtaining the residual stress of thin films and narrow areas, respectively.

### 3.6 Topography

Dislocations can be observed by applying TEM to thin ( $< 0.1 \mu\text{m}$ ) cross-sections of the sample. However, there is very little chance of our being able to observe the dislocations unless the density exceeds  $10^3$  to  $10^4/\text{cm}^2$ . For a single crystal with a low dislocation density, topography is useful. On a photograph that was obtained by exposing some of the Bragg reflection to the film, we can observe the defects as points of bright contrast. This is due to the extinction effect of the dynamical theory, by which Bragg reflection from a perfect crystal is weakened. The contrast also depends on many other factors such as X-ray beam divergence or the quality of a single crystal. The reflection (Bragg) method yields defects at the surface, while the transmission (Laue) method yields defects inside the crystal. It has been demonstrated that a micropipe in 6H SiC is a screw dislocation for which the burger's vector is as large as  $2c$  to  $7c$  (where  $c$  is a lattice constant of 6H SiC), using synchrotron white beam X-ray topography (SWBXT).<sup>25)</sup> The resolution (the size of the smallest observable defect) is limited by the method of image recording and is currently about 5  $\mu\text{m}$ . Ohsawa et al.<sup>26)</sup> have been attempting to improve the resolution of this method, and have managed to attain 1  $\mu\text{m}$ .

### 3.7 X-ray standing wave (XSW)<sup>3,4)</sup>

When an X-ray Bragg reflection is established in a crystal, the incident and reflected waves interfere to produce an X-ray standing wave in the crystal (dynamical theory). The intensity of the standing wave at a particular position can be changed by altering either the reflection angle, or the X-ray energy. The intensity of the photoelectrons, Auger electrons and the fluorescence of an atom attached to the surface are then monitored. The variation of the intensity caused by the angle or the energy can provide information on the adsorption site.

---

## 4. Scattering

### 4.1 Small-angle X-ray scattering

Small-angle X-ray scattering (SAXS) reflects non-

homogeneous electron density fluctuation. In the Guinier region, we can obtain the radius of gyration, while in the Porod region we can obtain the surface area. If the intensity  $I(q)$  has a peak, one can obtain the size of a molecule by Fourier transformation. To identify very small changes in the samples, highly-monochromatized X-ray beams with very little divergence are necessary. SR is ideally suited to such applications.

Although light scattering has been used to probe from 10 nm to 1  $\mu\text{m}$ , it cannot be applied to thick solutions or opaque samples. In an attempt to overcome this problem, ultra-small X-ray scattering (USAXS) using a Bonse-Hart double-crystal setup has been proposed. USAXS using SR led to whole new insights in materials science. Imaging with a 1- $\mu\text{m}$  resolution was attained using this method, and it has been used to observe creep cavities in copper metal.<sup>10, 27)</sup>

Grazing incidence small angle X-ray scattering (GISAXS) uses reflection geometry to perform SAXS. Omote<sup>28)</sup> measured the distribution of the pore sizes in porous low- $k$  film (methylsilsequioxane (600 nm) on an Si substrate) using a laboratory X-ray source, and determined the mean size to be 1.4 nm. Using SR, the scattered intensity has been recorded using two-dimensional detectors. Nano-scale structure characterization such as that of granular films or quantum dots<sup>29)</sup> has been investigated using this method.

#### 4.2 X-ray raman scattering

Laser raman scattering is one variety of inelastic light scattering, where light interacts with the lattice vibration. X-ray Raman scattering (XRS) is inelastic X-ray scattering that is caused by an electronic transition. It is analogous to electron energy loss spectroscopy (EELS). XRS may prove invaluable for investigating the chemical state of light elements under a gaseous atmosphere, because the XAFS method for light elements requires a vacuum.

---

### 5. X-ray absorption fine structure (XAFS)<sup>30)</sup>

---

The fine structure revealed by the X-ray absorption edge profile can be divided into two regions. X-ray absorption near edge structure (XANES) involves the absorption of incident photons (X-rays) such that the core electron is

excited to an empty excited state. This is the same process as that observed with the UV-VIS spectrum. The main difference from UV-VIS is that the electron is initially in the valence band, not the inner shell. Extended X-ray absorption fine structure (EXAFS) involves the oscillation of X-ray absorption, which is caused by the electron waves scattered from the atoms around that in question. The XANES spectrum yields the chemical state of the absorbing atom. The EXAFS spectrum, on the other hand, gives us the local structure surrounding the absorbing atom (radial distribution function). The XAFS spectrum can be simulated from a local structure model, and fitting the simulated spectrum to the experimental one refines that model. The energy tunability of SR has led to XAFS becoming a common tool for structure analysis. The applicability to amorphous as well as crystalline materials is a major advantage of the XAFS method. Furthermore, XAFS can be applied to the minority elements in a multi-component system. Therefore, the use of XAFS is indispensable in multi-component systems such as heterogeneous catalysis.

There are several practical methods for obtaining the XAFS spectrum. Transmitting geometry, in which transmitted X-rays are detected behind the sample, is the most common. The spectrum of the yield of the fluorescence X-rays or Auger electrons also reveals a fine structure near the absorption edge. The fluorescence method is often used to obtain the XAFS spectrum of a small amount of an element. The total electron yield gives us surface information up to a depth of several hundred nm. The capacitance of a Schottky diode is measured as a function of the incident X-ray energy. Because of the high sensitivity to relatively deep atoms, the spectrum obtained by capacitance-XAFS (C-XAFS) provides us with site-specific information. Another XAFS method involves observing a given Bragg reflection. This technique is called diffraction anomalous fine structure (DAFS). Only those atoms that contribute to the Bragg reflection are probed, although this is difficult to achieve, because the detector angle must be changed according to the Bragg angle to alter the incident X-ray energy.

Because of the high brilliancy of SR, the XAFS spectrum can be obtained in relatively little time. It

is necessary, however, to apply some special methods to the acquisition of the short time spectra which enables the observation of the rapid changes in the sample. These methods are: quick-XAFS (QXAFS) and dispersive-XAFS (DXAFS). In QXAFS, a monochromator sweeps continuously at high speed. In DXAFS, on the other hand, a polychromator is used to disperse the incident white beam into a fan shape with a continuously varying energy, and a two-dimensional detector obtains the intensity of the beam that is transmitted through the specimen. DXAFS allows us to observe transient states that exist for no more than a few milliseconds. A disadvantage of this method is that, currently, it can only be applied to transmission geometry. To make this method more useful, the extension of DXAFS experimental mode to fluorescence detection will be necessary.

Although EXAFS has been used to analyze the local structures surrounding a given atom, atomic-XAFS has been used to represent the electronic state of the atom itself. This technique is expected to be used for measuring the metal-support interaction in heterogeneous catalytic systems.<sup>31-35)</sup>

---

## 6. Fluorescence

---

The high brilliance of SR is also advantageous for the fluorescence X-ray detection of trace elements. Because of the tunability of SR, it may be possible to eliminate disturbances by overlapping any co-existing element signals. In the case of total reflection X-ray fluorescence (TRXF) detection, the limit on the heavy metal contamination of an Si wafer is improved by two decades, as compared with conventional laboratory experiments. The lower limit of detection (LLD) using Ge-SDD has reached the order of  $10^8$  atoms/cm<sup>2</sup>.<sup>36)</sup> ESRF has established an automated means of obtaining the TRXF, and is already offering a commercial service. The results of heavy element mapping on an Si wafer can be provided to a customer within two or three weeks.

---

## 7. Imaging

---

TEM provides us with an internal resolution of 1 nm. But the conditions required to make these observations, such as a vacuum and a thin specimen, restrict the technique's applicability. Although SEM

does not demand a thin specimen, it does require a vacuum. Further, we can only observe the surface of the specimen. Alternatively, we can use an optical microscope to observe samples in a gaseous atmosphere, but the resolution is limited. Therefore, we must explore the possibility of X-ray imaging to overcome these difficulties.

It is possible to create a three-dimensional reconstruction of a complex structure with a spatial resolution of 1  $\mu\text{m}$ , from the images obtained at different orientations of the sample with respect to the beam (computed tomography, CT). The detector, which was specially developed for these experiments, mainly determines the spatial resolution. In ID19 (ESRF), a combination of an X-ray to visible light converter screen, visible light optics, and a cooled CCD camera (FRELON, for Fast REad-out, LOw Noise), has been applied to many kinds of observations.

The SR light makes it possible to realize phase contrast imaging techniques. If we compare the phase shift and absorption in materials consisting of light elements, the phase shift surpasses the absorption, and this tendency increases as the energy of the X-rays increases. There are two approaches to phase contrast imaging. One involves using an X-ray interferometer, while the other uses refraction imaging.<sup>7, 37)</sup>

---

## 8. Micro beam

---

Currently, an SR micro beam can be formed in any of three different ways. A Fresnel zone plate (FZP) is a circular transmission diffraction grating consisting of alternate opaque and transparent rings. The FZP has a high level of transmittance, so is still being developed for use in the hard X-ray region. Therefore, it is mainly used in the soft X-ray region. The second method involves using a total reflection mirror. The curved total reflection mirror acts as lens for the X-rays. An elliptical mirror converges in one direction. A bent cylindrical mirror converges in two directions. So, the use of this method will cause parallelism to be lost as a result of the convergence. The third method involves the use of perfect-crystal X-ray optics. It is possible to compress the beam size by using the asymmetric Bragg reflection from a perfect crystal, while still

maintaining the parallelism. Except in the case of the total reflection mirror, the focal length changes according to the incident X-ray energy, therefore one has to add a mechanism for adjusting the sample position when performing a micro XAFS experiment.

The micro beam designed by Hasegawa and Hirai<sup>38)</sup> at BL16XU (SPring-8) consists of a bent-cylindrical pre-focusing mirror and elliptical mirrors in a Kirkpatrick-Baez configuration. The energy can be varied between 7 and 13 keV. The minimum size of the micro beam is  $0.45 \mu\text{m} \times 0.52 \mu\text{m}$ . This has been used for scanning fluorescence X-ray microscopy, micro diffraction, and micro XAFS.

Tsusaka et al.<sup>39)</sup> developed an X-ray micro beam ( $7.1 \mu\text{m} \times 4.8 \mu\text{m}$ ) with a low angular and energy divergence by applying perfect-crystal X-ray optics to BL24XU (SPring-8). The low angular divergence of about  $7.7 \mu\text{rad}$  and the low energy bandwidth of about 66 meV (at 15 keV) of this X-ray micro beam make it capable of detecting very small distortions in the crystal lattice  $\Delta d/d \sim 10^{-6}$ . Using this micro beam, Kimura et al.<sup>40)</sup> found that the compositions of  $\text{In}_x\text{Ga}_{1-x}\text{As}_y\text{P}_{1-y}$  on (100) InP during selective metal-organic vapor phase epitaxy change as the mask ( $\text{SiO}_2$ ) width is increased from 4 to  $40 \mu\text{m}$ .

## 9. Conclusion

The main characteristics of SR are its tunability, high level of orientation, and high intensity. Among the many experimental methods using SR, XAFS is especially useful when compared with conventional laboratory method. The reason for this is the fact that two of the technique's characteristics, namely, tunability and high intensity, are extremely important to the XAFS method. By using the XAFS method, we can observe local structures including information on neighboring atoms around a given element (atom). This is applicable to amorphous materials and solutions as well as crystalline materials. To date, many experiments have been done using the XAFS method with SR. By using a variety of methods including XAFS, we can observe the structure or composition in narrow areas or monolayers, thanks to the characteristics of SR such as its brilliance. Researchers who are facing difficulties due to the limits imposed by

conventional experimental techniques are urged to consider X-ray analysis using SR.

## References

- 1) Kikuta, S. : *X-senn Kaisetsu Sannrann Gijyutsu*, Vol. 1 (in Japanese), (1992), 274, Univ. Tokyo Press
- 2) *Sinnkurotoronn Housyakou no Kiso*, Oyanagi, H. ed., (in Japanese), (1996), 608, Maruzen
- 3) *Nanoerekutoronikusu wo Sasaeru Zairyuu Kaiseki*, Ojima, S. and Honma, Y., eds., (in Japanese), (1996), 275, Inst. Elec. Inf. Commun. Eng.
- 4) *Kessyo Kaiseki Handobukku*, Harada, J. et al., eds., (in Japanese), (1999), 673, Kyoritsu
- 5) *X-senn Ketsuzou Kougaku*, Namioka, T. and Yamashita, K., eds., (in Japanese), (1999), 309, Baifukan
- 6) *Atarasii Housyakou no Kagaku*, Sugano, S., et al., eds., (in Japanese), (2000), 233, Kodansha
- 8) *Kouzou Kaiseki*, Fujii, Y., ed., (in Japanese), (2001), 378, Maruzen
- 7) *Kyokugenn Jyoutai wo Miru Housyakou Anarisisu*, Oshima, M., ed., (in Japanese), (2002), 214, Jpn. Sci. Soc. Press
- 9) Jordan-Sweet, J. L. : *IBM J. Res. Develop.*, **44** (2000), 457
- 10) Long, G. A., et al. : *J. Res. Natl. Inst. Stand. Technol.*, **106**(2001), 1141
- 11) Sasaki, S., et al. : "Special Issue – Frontiers in Crystallography with Synchrotron Radiation", *J. Cryst. Soc. Jpn.*, **39**(1997), 1-142 (in Japanese)
- 12) Suematsu, H., et al. : "Special Issue: Recent Development of Structural Materials Science by Synchrotron X-ray", *Solid State Phys.*, **37**(2002), 581-725 (in Japanese)
- 13) *Funnmatsu X-senn Kaiseki no Jissai*, Jpn. Soc. Anal. Chem., ed., (in Japanese), (2002), 196, Asakura
- 14) Takata, M., et al. : *Nature (London)*, **377**(1995), 46
- 15) Takata, M., et al. : *New Diamond and Frontier Carbon Technology*, **12**(2002), 271
- 16) Robinson, I. K. : *Phys. Rev. B*, **33**(1986), 3830
- 17) Tabuchi, M., et al. : *J. Cryst. Growth*, **237/239** (2002), 1133
- 18) *Hyomenn Dennshi Kaisetsuhou*, Surface Sci. Soc. of Jpn., ed., (in Japanese), (2003), 171, Maruzen
- 19) Renaud, G. : *Surface Sci. Rep.*, No.32(1998), 1
- 20) Robinson, I. K. and Tweet, D. J. : *Rep. Prog. Phys.*, **55**(1992), 599
- 21) Semicond. Ind. Assoc. : "Int. Technol. Roadmap for Semicond. 2001 Ed.", (online), available from <<http://public.itrs.net/>>, (accessed 2003-5-16)
- 22) Awaji, N., et al. : *SPring-8 User Experiment Rep. No.9* (2002A), 290
- 23) Awaji, N. : *FUJITSU Sci. Tech. J.*, **38**(2002), 82
- 24) Reimers, W., et al. : *J. Mat. Sci. Lett.*, **18**(1999), 581
- 25) Huang, X. R., et al. : *Appl. Phys. Lett.*, **74**(1999), 353-355
- 26) Tanuma, R., et al. : *SPring-8 User Experiment Rep. No.9* (2002A) 284

- 27) Long, G. G. : Mater. Sci. Eng. A, **309/310**(2001), 28
- 28) *X-senn Bunseki no Shinnpo*, Omote, K and Itoh, Y.,  
(in Japanese), No.33(2002), 185
- 29) Okuda, H. and Ochiai, S. : Photon Factory News,  
No.20(2003), 24 (in Japanese)
- 30) *X-senn Kyuusyuu Bunnkouhou*, Ohta, T., ed.,  
(in Japanese), (2002), 294, Ind. Pub. & Consulting  
Inc.
- 31) Holland, B. W. : J. Phys. C, **11**(1978), 633
- 32) Rehr, J. J. : Phys. Rev. B, **49**(1994), 12347
- 33) Mojet, B. L., et al. : J. Catal., **186**(1999), 373
- 34) Koningsberger, D. C., et al. : Topics in Catal.  
**10**(2000), 143
- 35) Ramaker, D. E., et al. : J. Catal., **203**(2001), 7
- 36) Awaji, N., et al. : Jpn. J. Appl. Phys., **39**(2000),  
L1252
- 37) Cloetens, P., et al. : Europhys. News, **32**(2001), 46
- 38) Hasegawa, M. and Hirai, Y. : J. Appl. Phys.,  
**90**(2001), 2792
- 39) Tsusaka, Y., et al. : Jpn. J. Appl. Phys., Part 2  
**39**(2000), L635
- 40) Kimura, S., et al. : Appl. Phys. Lett., **77**(2000), 1286  
(Report received on Apr. 23, 2003)



---

**Yoshiharu Hirose**

Year of birth : 1950

Division : Mater. Analysis & Evaluation  
Div.Research fields : Materials analysis using  
synchrotron radiation, Surface  
analysisAcademic society : Phys. Soc. of Jpn.,  
Chem. Soc. of Jpn., Surface Sci.  
Soc. of Jpn.